Stability Evaluation and System Identification of Flexible Multibody Systems*

Olivier A. Bauchau and Jielong Wang.
Daniel Guggenheim School of Aerospace Engineering,
Georgia Institute of Technology,
Atlanta, GA, USA.

Abstract

This paper is concerned with the linearized stability analysis and system identification of flexible multibody systems. Two closely related stability analysis approaches are summarized. Next, these approaches are extended to provide robust system identification procedures that combine least squares techniques and Kalman filters. The singular value decomposition, a numerically stable mathematical tool, is used to improve the robustness of the algorithm. The proposed algorithm identifies a minimum order plant based on input-output data, and is applicable to both experimental measurements or numerically computed responses. The proposed approaches are computationally inexpensive and consist of purely post processing steps that can be used with any multi-physics computational multibody tool or with experimental data.

1 Introduction

The problem of system realization or system identification for linear time-invariant models has received considerable attention in numerous engineering applications such as dynamic simulation and control of flight vehicle, identification of vibrational modes of large-scale flexible structures, the health monitoring and damage detection of civil engineering structures, or electrical circuits and imaging processes. In general, system identification aims at creating a mathematical model of a dynamical system from measurements of its input and output. In past decades, identification tools for the construction of state space representation of linear systems have been developed. However, more work is needed to develop identification procedures for complex, multi-physics, flexible multibody systems. Review papers have been presented on the subject of system identification: Kim and Arora [1] focused on linear and nonlinear dynamical systems, and a number of authors [2] reviewed subspace-based identification methods.

*Submitted for publication in *Multibody System Dynamics,* 2007.

The seminal work Kalman [3] introduced the concepts of controllability and observability, which are important prerequisites to identification. A state space approach was subsequently provided by the Ho-Kalman algorithm [4], and a minimum realization was obtained from Markov parameters. This algorithm is widely used as an identification algorithm, but it also contributed to the development of state space models [5] presenting balanced properties. When used in conjunction with numerically stable tools such as the singular value decomposition, the Ho-Kalman algorithm has been extended to the eigensystem realization algorithm [6]. To decrease the effects of noise and nonlinearities, the eigensystem realization algorithm with data correlation was developed. Furthermore, eigensystem realization algorithm combined with observer/Kalman filter identification became an optimal procedure to construct a minimum order plant and compute Kalman filter gain matrix from input-output data. However, the computation of Markov parameters by observer/Kalman filter identification remains complex and determines the accuracy of the system realization. If a poor approximation of Markov parameters is obtained, the system identification might be meaningless, prompting the development of methods aimed at improving the accuracy of these parameters. System realization methods based on Ho-Kalman algorithms and their extensions are known as minimum realization procedures.

Another system identification approach is based on subspace identification methods [7]. In these methods, a state space representation of a linear system is found by matrix projection operations, and eliminating the effects of noise is a major concern. For stochastic systems, Peeters and de Roeck [8] have used Kalman filters to eliminate the effect of white noise with zero mean. For more general cases, Overschee and de Moor [7] have reviewed subspace methods and algorithms for the identification of linear time-invariant systems from given input-output data. Robust identification procedures have been developed for deterministic, stochastic, and combined deterministic-stochastic systems. Because matrix projection operations are computationally expensive, these methods are most suitable for solving small size problems.

This paper focuses on a modified minimum realization approach combined with least squares techniques, for the analysis of nonlinear, flexible multibody systems. The linearized realization is valid for small perturbations about an equilibrium configuration of the nonlinear system. *Similarity transformation* and *balanced truncation* form the theoretical basis for the proposed identification algorithm. Similarity transformations clearly do not affect system input-output behavior. This implies that the linear time-invariant model of the system is not unique. Balanced truncations [5, 9] dramatically decrease the order of high-dimensional systems; the modes of the reduced model form a subset of the modes of the original system and remain invariant in this reduction procedure.

The goal of this work is to develop robust identification algorithms to construct linearized plant models from known control inputs and sensed system output data. The identified linearized plant models must be suitable for the solution of optimal control problems. The proposed algorithms can be applied to one or

multiple time signals, and are equally applicable to experimental measurements or numerically computed responses. For linear systems, the signals are measured from the dynamic responses directly; for nonlinear systems, the signals are computed as the difference between the sensed responses under external perturbations and those of the equilibrium configuration.

The proposed system identification algorithm uniquely combines the methods of minimum realization and subspace identification. The proposed approach bypasses the computation of Markov parameters because the free impulse response of the system can be directly computed in the present computational environment. As proposed by Bauchau and Wang [10, 11] for stability analysis, minimum realization concepts were applied to identify the stability and output matrices. The singular value decomposition, a numerically stable mathematical tool, is used to minimize the effects of noise. On the other hand, subspace identification algorithms construct a state space plant model of linear system by using computational expensive oblique matrix projection operations. The proposed algorithm avoids this burden by computing the Kalman filter gain matrix and model dependency on external inputs based on a small sized subspace. The Kalman filter gain matrix is determined by solving the discrete time algebraic Riccati equation. Both deterministic or combined deterministic-stochastic systems can be treated. Finally, the least squares technique is applied to compute the model dependency on external inputs.

This paper first summarizes two stability analysis approaches based on the partial Floquet and autoregressive algorithms. Next, these methods are extended to provide robust system identification algorithms. Finally, numerical examples validate the proposed approach.

2 Stability analysis algorithms

The stability analysis approach developed by Bauchau and Wang [10, 11] is briefly summarized here. The output Hankel matrix, Y_k, defined as,

$$Y_k = \begin{bmatrix} \underline{y}_k & \underline{y}_{k+1} & \cdots & \underline{y}_{k+n-1} \\ \underline{y}_{k+1} & \underline{y}_{k+2} & \cdots & \underline{y}_{k+n} \\ \vdots & \vdots & \ddots & \vdots \\ \underline{y}_{k+m-1} & \underline{y}_{k+m} & \cdots & \underline{y}_{k+m+n-2} \end{bmatrix}, \tag{1}$$

plays an important role in the analysis. It is an assembly of the time histories of the output sensors, $\underline{y}_k$. To simplify the description of the algorithm, a single input-single output system is considered here. In this case, array $\underline{y}_k$ consists of a single entry. The relationship between the states of the system at two consecutive time instants is expressed in terms of the *transition matrix*, Q, such that $Y_1 = Q\, Y_0$. This relationship does not allow the exact computation of the transition matrix due to the fact that only limited information is available. An approximation to the transition matrix is evaluated as $Q = Y_1 Y_0^+$,

where Y_0^+ indicates the Moore-Penrose generalized inverse [12] of Y_0, which can be evaluated using the singular value decomposition as $Y_0^+ = V_r \Sigma_r^{-1} U_r^T$, where r is the estimated rank of Y_0. The estimated transition matrix becomes $Q_{(m\times m)} = Y_1 V_r \Sigma_r^{-1} U_r^T$. Consequently, it makes sense to project matrix Q in the subspace defined by the r proper orthogonal modes of Y_0, stored in U_r, to find $\hat{Q}_{(r\times r)} = U_r^T Q\ U_r = U_r^T Y_1 V_r \Sigma_r^{-1}$. If the eigenvalue decompositions of Q and $\hat{Q}$ can be written as $Q = R\ e^{\lambda \Delta t} R^{-1}$ and $\hat{Q} = \hat{R}\ e^{\lambda \Delta t} \hat{R}^{-1}$, the eigenvalues of transition matrix are $\exp(\lambda_j \Delta t), j = 1, 2, \ldots, m$ and assumed to be distinct in this discussion. The system is stable if and only if the norms of all eigenvalues are smaller than unity: $|\exp(\lambda_j \Delta t)| < 1, j = 1, 2, \ldots, m$. The stability analysis involves the determination of the characteristic exponents of the system from the eigenvalues of the transition matrix. A typical eigenvalue is written as $\exp(\lambda_j \Delta t) = r_j \exp(\pm \mathbf{i} \phi_j)$, where $\mathbf{i} = \sqrt{-1}$, and a characteristic exponent as $\lambda_j = \omega_j[\zeta_j \pm \mathbf{i}\sqrt{1-\zeta_j^2}]$, where ω_j and ζ_j are the frequency and damping, respectively, associated with this characteristic exponent; it then follows that

$$\zeta_j = \frac{c_j}{\sqrt{1+c_j^2}}; \quad \omega_j = \frac{\ln r_j}{\zeta_j \Delta t}, \quad j = 1, 2, \ldots, m/2, \tag{2}$$

where $c_j = (\ln r_j)/\phi_j$.

The autoregressive method is similar to the approach presented above. The relationship between the states of the system at two consecutive time instants is expressed in terms of the autoregressive matrix B as $Y_1 = Y_0 B$. Clearly, matrix B and the transition matrix Q are closely related since $B = Y_0^+ Q Y_0$. Here again, the Moore-Penrose generalized inverse of matrix Y_0 is used to evaluate an approximation of this matrix as $B = Y_0^+ Y_1$, and finally, $B_{(n\times n)} = V_r \Sigma_r^{-1} U_r^T Y_1$. In view of highly redundant nature of the data stored in matrix Y_0, it should be expected that, in general, $r < n$, and hence, only r eigenvalues of B should be physically meaningful. Consequently, it makes sense to project matrix B in the subspace defined by V_r, to find $\hat{B}_{(r\times r)} = V_r^T B V_r = \Sigma_r^{-1} U_r^T Y_1 V_r$. All the formulations of Q, $\hat{Q}$, B and $\hat{B}$ can be used to extract the valuable information as to the stability characteristics of the linear or linearized system.

3 The robust system identification algorithm

The system identification algorithm is an extension of the stability analysis approaches summarized in the previous section. To improve the robustness of the algorithm, the least squares and Kalman filter techniques are applied. The systems to be investigated here are assumed to be linearized models of nonlinear multibody systems; typically, the behavior of small perturbations about an equilibrium configuration is investigated. To account for the effects of white noise, a combined deterministic-stochastic model is considered, and modeled by a set of

high-dimensional equations

$$\underline{u}_{k+1} = A_s \underline{u}_k + B_s \underline{f}_k + \underline{w}_k \quad \text{and} \quad \underline{y}_k = C\underline{u}_k + D\underline{f}_k + \underline{v}_k, \tag{3}$$

where $\underline{u}_{k\ (2N)}$ is the state vector storing the displacements and velocities of all degrees of freedom of the model at time $t = k\Delta t$, $\underline{f}_{k(N_c)}$ is the array of control inputs, and $\underline{y}_{k(N_s)}$ the array of system outputs. Matrices $A_{s(2N\times 2N)}$, $B_{s(2N\times N_c)}$, $C_{(N_s\times 2N)}$, and $D_{(N_s\times N_c)}$ are constant coefficient matrices that define the system; the subscripts indicate the size of the corresponding arrays. Matrix A_s, called the stability matrix of the system, contains the information concerning the stability of the system. Vector $\underline{w}_k$ represents noise in the state vector, assumed to be Gaussian with a zero mean, stationary and white, whereas vector $\underline{v}_k$ represents measurement noise, assumed to share the same characteristics. The covariance matrix is defined as

$$E(\left| \begin{array}{c} \underline{w}_i \\ \underline{v}_i \end{array} \right| \lfloor \begin{array}{cc} \underline{w}_j^T & \underline{v}_j^T \end{array} \rfloor) = \left[\begin{array}{cc} E_w & E_s \\ E_s^T & E_v \end{array} \right] \delta_{ij}, \tag{4}$$

where δ_{ij} is the Kronecker delta. In view of the above assumptions, $E(\underline{w}_k) = 0$, and $E(\underline{v}_k) = 0$.

The object of system identification is to determine the system matrices, A_s, B_s, C and D, the covariance matrices E_w, E_s and E_v, and the Kalman filter gain matrix, K, to construct the forward innovation model

$$\bar{\underline{u}}_{k+1} = A_s \bar{\underline{u}}_k + B_s \underline{f}_k + K\underline{\epsilon}_k \quad \text{and} \quad \underline{y}_k = C\bar{\underline{u}}_k + D\underline{f}_k + \underline{\epsilon}_k, \tag{5}$$

where $\bar{\underline{u}}_{k+1}$ are the filtered states, and $\underline{\epsilon}_k$ the output residual white noise of zero mean.

The system is excited for the first m time steps by control inputs $\underline{f}_k$; no control input are applied for the subsequent time steps. After m time steps, the inputs vanish and the forward innovation model reduces to

$$\bar{\underline{u}}_{k+1} = A_s \bar{\underline{u}}_k + K\underline{\epsilon}_k \quad \text{and} \quad \underline{y}_k = C\bar{\underline{u}}_k + \underline{\epsilon}_k. \tag{6}$$

Juang [13] has proved $\underline{\epsilon}_k$ is white noise with zero mean whether the state noise, $\underline{w}_k$, and measurement noise, $\underline{v}_k$, are white noise or not. The free impulse response of the linearized model of nonlinear multibody system, $\underline{y}_k$, is obtained either from numerical simulation, or from experimental data. In view of eqs. (6), this response can be written as the following convolution

$$\underline{y}_k = CA_s^k \bar{\underline{u}}_0 + \sum_{j=0}^{k-1} CA_s^{k-1-j} K\underline{\epsilon}_j + \underline{\epsilon}_k. \tag{7}$$

This result will be recast in a matrix form by defining the following notation: the filtered state array, $\bar{U}_k$,

$$\bar{U}_k = \left[\begin{array}{cccc} \bar{\underline{u}}_k & \bar{\underline{u}}_{k+1} & \cdots & \bar{\underline{u}}_{k+n-1} \end{array} \right], \tag{8}$$

and residual noise Hankel matrix, E_k,

$$E_k = \begin{bmatrix} \underline{\epsilon}_{k+m-1} & \underline{\epsilon}_{k+m} & \cdots & \underline{\epsilon}_{k+m+n-2} \\ \underline{\epsilon}_{k+m-2} & \underline{\epsilon}_{k+m-1} & \cdots & \underline{\epsilon}_{k+m+n-3} \\ \cdots & \cdots & \ddots & \cdots \\ \underline{\epsilon}_{k} & \underline{\epsilon}_{k+1} & \cdots & \underline{\epsilon}_{k+n-1} \end{bmatrix}. \tag{9}$$

For $k = m$, eqs. (7) are now written as

$$Y_m = M_o \bar{U}_m + \mathcal{K}_0 E_m; \tag{10a}$$
$$\bar{U}_m = A_s^m \bar{U}_0 + M_{\mathcal{K}} E_0, \tag{10b}$$

where the observability matrix, M_o, is defined as $M_o = \lfloor C^T \; {A_s}^T C^T \; \ldots \; {A_s^{m-1}}^T C^T \rfloor^T$, and the following two matrices were defined

$$M_{\mathcal{K}} = \begin{bmatrix} K & A_s K & A_s^2 K & \ldots & A_s^{m-1} K \end{bmatrix}, \tag{11}$$

$$\mathcal{K}_0 = \begin{bmatrix} 0 & 0 & \ldots & 0 & 0 & I \\ 0 & 0 & \ldots & 0 & I & CK \\ 0 & 0 & \ldots & I & CK & CA_sK \\ \vdots & \vdots & \ddots & \vdots & \vdots & \vdots \\ I & CK & \ldots & CA_s^{m-4}K & CA_s^{m-3}K & CA_s^{m-2}K \end{bmatrix}. \tag{12}$$

With the help of eq. (10a), it is now possible to evaluate the data correlation matrix, $Y_m Y_0^T = M_o \bar{U}_m Y_0^T + \mathcal{K}_0 E_m Y_0^T$, where the last term vanishes since the white noise assumption implies $E_m Y_0^T = 0$. For time step $m+1$, eq. (10a) becomes $Y_{m+1} = M_o \bar{U}_{m+1} + \mathcal{K}_0 E_{m+1}$. Next, the first equation of eqs. (6) implies $\bar{U}_{m+1} = A_s \bar{U}_m + K \begin{bmatrix} \underline{\epsilon}_m & \underline{\epsilon}_{m+1} & \cdots & \underline{\epsilon}_{m+n-1} \end{bmatrix}$; introducing this result in the previous equation yields $Y_{m+1} = M_o A_s \bar{U}_m + \widetilde{\mathcal{K}}_0 \widetilde{E}_m$, where $\widetilde{\mathcal{K}}_0$ is defined as

$$\widetilde{\mathcal{K}}_0 = \begin{bmatrix} 0 & 0 & \ldots & 0 & 0 & I & CK \\ 0 & 0 & \ldots & 0 & I & CK & CA_sK \\ 0 & 0 & \ldots & I & CK & CA_sK & CA_s^2K \\ \vdots & \vdots & \ddots & \vdots & \vdots & \vdots & \vdots \\ I & CK & \ldots & CA_s^{m-4}K & CA_s^{m-3}K & CA_s^{m-2}K & CA_s^{m-1}K \end{bmatrix}, \tag{13}$$

and $\widetilde{E}_m$ as

$$\widetilde{E}_m = \begin{bmatrix} \underline{\epsilon}_{2m} & \underline{\epsilon}_{2m+1} & \cdots & \underline{\epsilon}_{2m+n-1} \\ \underline{\epsilon}_{2m-1} & \underline{\epsilon}_{2m} & \cdots & \underline{\epsilon}_{2m+n-2} \\ \cdots & \cdots & \vdots & \cdots \\ \underline{\epsilon}_{m} & \underline{\epsilon}_{m+1} & \cdots & \underline{\epsilon}_{m+n-1} \end{bmatrix}. \tag{14}$$

Now, the data correlation matrix at time step $m+1$ is evaluated as $Y_{m+1} Y_0^T = M_o A_s \bar{U}_m Y_0^T + \widetilde{\mathcal{K}}_0 \widetilde{E}_m Y_0^T$, where the last term vanishes here again since the white

noise assumption implies $\widetilde{E}_m Y_0^T = 0$. The following notation is introduced to denote the data correlation matrices

$$\mathcal{O}_0 = Y_m Y_0^T = M_o \bar{U}_m Y_0^T \quad \text{and} \quad \mathcal{O}_1 = Y_{m+1} Y_0^T = M_o A_s \bar{U}_m Y_0^T. \tag{15}$$

A truncated factorization of matrix $\mathcal{O}_0$ is evaluated by means of the singular value decomposition to find $\mathcal{O}_0 = U_r \Sigma_r V_r^T$, where r is the estimated rank of $\mathcal{O}_0$. Since $\mathcal{O}_0 = M_o \bar{U}_m Y_0^T = U_r \Sigma_r^{1/2} \Sigma_r^{1/2} V_r^T$, the observability matrix, M_o, is selected as $M_o = U_r \Sigma_r^{1/2}$, and the matrix product, $\bar{U}_m Y_0^T$, as $\bar{U}_m Y_0^T = \Sigma_r^{1/2} V_r^T$. The stability matrix, A_s, is now computed from the second equation of eqs. (15) as $A_s = \Sigma_r^{-1/2} U_r^T \mathcal{O}_1 V_r \Sigma_r^{-1/2}$. Next, matrix C is determined from the first N_s rows of observability matrix, M_o.

The computation of the Kalman filter gain requires the covariance matrices E_w, E_s, and E_v. The projection of the rows of matrix Y_k onto the rows of matrix Y_0 is $Y_k^{\parallel} = Y_k Y_0^T \left(Y_0 Y_0^T\right)^+ Y_0$. The theorem of stochastic subspace identification [7] states that this projection can be represented as the product of the observability matrix and filtered states, *i.e.* $Y_k^{\parallel} = M_o \bar{U}_k$, and hence, $\bar{U}_k = \Sigma_r^{-1/2} U_r^T Y_k^{\parallel}$. Expressing this latter relationship for two consecutive time steps, m and $m+1$, gives $\bar{U}_m = \Sigma_r^{-1/2} U_r^T Y_m^{\parallel}$ and $\bar{U}_{m+1} = \Sigma_r^{-1/2} U_r^T Y_{m+1}^{\parallel}$. The forward innovation model, eqs. (6), is recast in matrix form as

$$\bar{U}_{m+1} = A_s \bar{U}_m + K \rho_v \quad \text{and} \quad \hat{Y}_m = C \bar{U}_m + \rho_v, \tag{16}$$

where array $\hat{Y}_m = [\underline{y}_m \ \underline{y}_{m+1} \ \cdots \ \underline{y}_{m+n-1}]$ and $\rho_v = [\underline{\epsilon}_m \ \underline{\epsilon}_{m+1} \ \cdots \ \underline{\epsilon}_{m+n-1}]$. Since the system matrices, A_s and C, and the filtered states, $\bar{U}_{m+1}$ and $\bar{U}_m$, are now known, the residuals, $K\rho_v$ and ρ_v, are easily evaluated from eqs.(16). Finally, the covariance matrices are estimated from the residuals

$$\begin{bmatrix} E_w & E_s \\ E_s^T & E_v \end{bmatrix} = \begin{bmatrix} K\rho_v \\ \rho_v \end{bmatrix} \left[(K\rho_v)^T \ \rho_v^T \right]. \tag{17}$$

It is now possible to compute the Kalman filter gain matrix, K, by solving a discrete time algebraic Riccati equations using a Schur-type algorithm [14]. Note that the computation of Kalman filter gain is left as a user option.

The last step of proposed system identification algorithm includes the determination of matrices B_s and D. Once all the other unknowns are found, the problem becomes linear in the unknowns B_s and D. The least squares regression is used to solve a redundant system of linear equations for rest of the unknowns. The forward innovation model, eqs. (5), is reformulated

$$\underline{\bar{u}}_{k+1} = K \underline{y}_k + \bar{A}_s \underline{\bar{u}}_k + (B_s - KD) \underline{f}_k \quad \text{and} \quad \underline{y}_k = C \underline{\bar{u}}_k + D \underline{f}_k + \underline{\epsilon}_k, \tag{18}$$

where the noise array $\underline{\epsilon}_k$ was eliminated from the first equation using the second equation of eqs. (5), and the closed-loop stability matrix $\bar{A}_s = A_s - KC$. The

solution of forward innovation model can be written here again as a convolution

$$\underline{y}_k = \sum_{j=0}^{k-1} C\bar{A}_s^{k-1-j} K \underline{y}_j + C\bar{A}_s^k \underline{u}_0 + \sum_{j=0}^{k-1} C\bar{A}_s^{k-1-j} \left(B_s - KD\right) \underline{f}_j + D\underline{f}_k + \underline{\epsilon}_k. \quad (19)$$

Furthermore, the system outputs, $\underline{y}_k$, are reformulated as linear functions of unknowns of $\underline{u}_0$, B_s and D, $\underline{y}_k = \underline{y}_k^K + \mathcal{A}_k \underline{\mathcal{B}} + \underline{\epsilon}_k$, the array $\mathcal{A}_k$ and vectors $\underline{y}_k^K$, $\underline{\mathcal{B}}$ are cast as

$$\begin{aligned} \mathcal{A}_k &= \left[\; C\bar{A}_s^k, \;\; \textstyle\sum_{j=0}^{k-1} \underline{f}_j^T \otimes C\bar{A}_s^{k-1-j}, \;\; \underline{f}_k^T \otimes I - \sum_{j=0}^{k-1} \underline{f}_j^T \otimes C\bar{A}_s^{k-1-j} K \; \right], \\ \underline{y}_k^K &= \sum_{j=0}^{k-1} C\bar{A}_s^{k-1-j} K \underline{y}_j \quad \text{and} \quad \underline{\mathcal{B}} = \left| \begin{array}{c} \underline{u}_0 \\ \text{vec}(B_s) \\ \text{vec}(D) \end{array} \right|, \end{aligned} \quad (20)$$

where $\otimes$ denotes the Kronecker product, and $\text{vec}(A)$ indicates the operation that constructs an array by stacking the columns of an arbitrary matrix A, note the identity, $\text{vec}(AXB) = (B^T \otimes A)\text{vec}(X)$, where A, X and B are arbitrary matrices [15]. Finally, the remaining unknowns, stored in array $\underline{\mathcal{B}}$, are obtained from a least squares approximation as

$$\underline{\mathcal{B}} = (\mathcal{A}_k^T \mathcal{A}_k)^{-1} \mathcal{A}_k^T (\underline{y}_k - \underline{y}_k^K). \quad (21)$$

Of course, the singular value decomposition could also be used to this effect.

In summary, the proposed procedure for system identification involves the following steps. *(1)* Assemble the output block Hankel matrices Y_0, Y_m and Y_{m+1}, eqs. (1), and compute the data correlation matrices $\mathcal{O}_0 = Y_m Y_0^T$ and $\mathcal{O}_1 = Y_{m+1} Y_0^T$. *(2)* Perform the singular value decomposition of data correlation matrix, $\mathcal{O}_0$, using Lanczos algorithm, $\mathcal{O}_0 = U_r \Sigma_r V_r^T$. Compute the observability matrix $M_o = U_r \Sigma_r^{1/2}$ and matrix product $\bar{U}_m Y_0^T = \Sigma_r^{1/2} V_r^T$. *(3)* Compute stability matrix, $A_s = \Sigma_r^{-1/2} U_r^T \mathcal{O}_1 V_r \Sigma_r^{-1/2}$. Matrix C is extracted as the first N_s rows of the observability matrix. *(4)* Compute the projections $Y_m^{\|} = Y_m Y_0^T \left(Y_0 Y_0^T\right)^+ Y_0$ and $Y_{m+1}^{\|} = Y_{m+1} Y_0^T \left(Y_0 Y_0^T\right)^+ Y_0$, and the filtered state sequences, $\bar{U}_m = \Sigma_r^{-1/2} U_r^T Y_m^{\|}$ and $\bar{U}_{m+1} = \Sigma_r^{-1/2} U_r^T Y_{m+1}^{\|}$. *(5)* Compute covariance matrices, E_w, E_s, and E_v, with eqs. (17), and determine the Kalman filter gain matrix, K, by solving a discrete time algebraic Riccati equations. *(6)* Compute matrices B_s and D by least squares approximation, see eqs. (21).

If dealing with a deterministic model, steps 4 and 5 can be bypassed, and the system matrices A_s, B_s, C and D are identified.

4 Numerical examples

Two examples will be presented to validate the proposed stability and system identification algorithms.

4.1 Identification of a wing-aileron system

The aeroelastic problem considers the flutter of a wing-aileron system, as depicted in fig. 1. The half wing has a rectangular planform of length $L_w = 20$ ft and chord length $c = 6$ ft. The flap of length $L_f = 3$ ft extends along the wing from stations 15 to 18 ft.

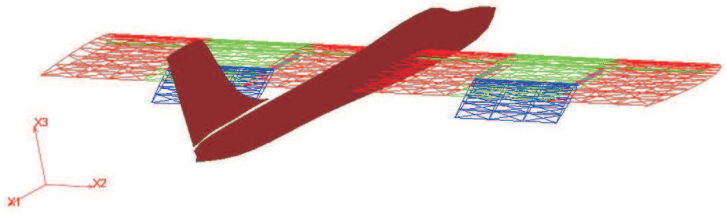

Figure 1: Configuration of the Wing-Aileron system

The structural properties of the flap are as follow: bending stiffness, $EI_f = 4.7\ 10^5$ lbs·ft^2, torsional stiffness, $GJ_f = 2.4\ 10^4$ lbs·ft^2, mass per unit span, $m_f = 0.75$ slugs/ft, polar moment of inertia, $I_f = 1.95$ slugs·ft. The flap is attached to the wing by means of two brackets of length $L_b = 3.1$ ft. On the inboard side, the flap is attached to the bracket by means of a revolute joint followed by a flexible joint and a universal joint. The flexible joint defines a torsional spring with stiffness $k_\theta = 10^6$ lb/ft, which models the stiffness of the flap control system. On the outboard side, the flap is attached to the wing with a prismatic joint followed by a spherical joint. These joints allow the wing and flap to deform independently. The finite element based multibody representation of the system involves a total of 1,072 structural and 28 aerodynamic states.

When the air flow reaches the speed of $U_f = 590$ ft/sec, the system becomes unstable. For model identification, two controls are used: the rotation of the flap, θ_f, and the angle of attack of the wing, θ_w.

The proposed system identification algorithm was used to construct a subspace plant model using four measurements: the transverse displacements and velocities at the tip and middle of the right wing, labeled as signal 1, 2, 3 and 4, respectively. To identify the system, the following control inputs were used: the flap deflection was prescribed as $\theta_f(t) = b_0 - b_0 \cos(10\pi t)$, for $t \in [0, 0.2]$ sec and $b_0 = 15$ degrees, whereas the wing angle of attack, θ_w, was prescribed as $\theta_w(t) = a_0 - a_0 \cos(10\pi t)$, for $t \in [0, 0.2]$ and $a_0 = 1$ degree. The dynamic simulation is run for a period of 0.55 sec with a constant time step size of 1 msec. In the singular value decomposition, a rank number of $r = 24$ was selected, and the minimum realization involved a state vector of size 24.

Once the system was identified, the accuracy of the reduced model was verified by comparing the predictions of the full and reduced models for different control inputs: the flap deflection was prescribed as $\theta_f(t) = b_0 - b_0(\cos(10\pi t) + \cos(5\pi t))$,

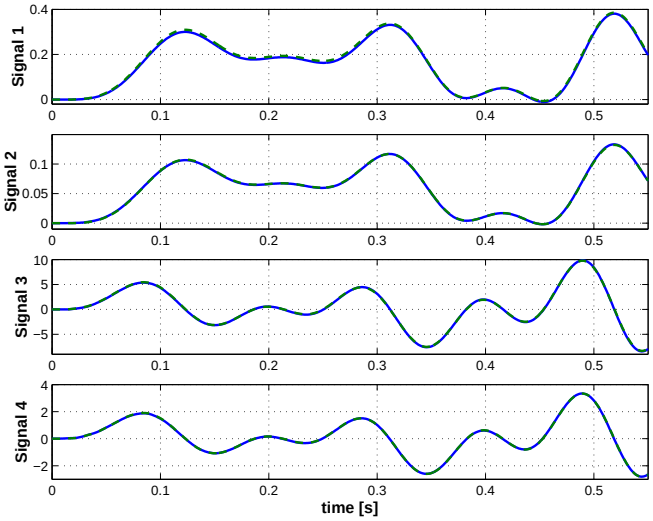

Figure 2: The input-output behavior approximation: original signal (solid line), reconstructed signal, (dashed line).

and the wing angle of attack as $\theta_w(t) = a_0 - a_0(\cos(10\pi t) + \cos(5\pi t))$, for a total period of 0.55 s. The predictions of the two models are compared in fig. 2. Excellent correlation is observed between the two predictions pointing to a robust identification of the system. Clearly, the plant model identified here is valid for the investigated frequency range, which is near the flutter frequency. If reduced order models valid over a wider frequency range are required, the frequency content of the excitation would need to be wider as well.

4.2 Trim analysis of helicopter rotor system

The second example deals with a detailed aeroelastic problem of a complex rotor system using a finite element based multibody dynamic simulation code [16]. The multibody representation includes the four rotor blades and control actuators. The description of the physical properties of each blade can be found in ref. [17]. The four blades are connected to the hub by means of root retention structures and lead-lag dampers. The configuration of the rotor system is shown in fig. 3.

This problem involves both structural and aerodynamic states. For structural modeling, each blade was discretized using ten cubic finite elements. The root retention, connected hub and blade, was separated into three segments and modeled by one, two and two beam elements, labeled segment 1, 2 and 3 in fig. 3. The flap, lead-lag and pith modes of the blade were described by three revolute joints connected the first two segments of the root retention structures. The prismatic joints were used to model the lead-lag dampers. The rotor was clamped to the ground at the center of the hub. The collective and cyclic angles of the blade

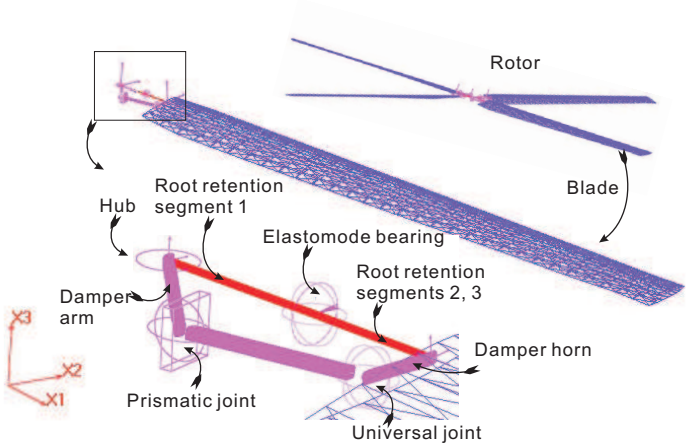

Figure 3: Schematic of the helicopter rotor system.

were controlled by prescribing the relative rotations of the pitch revolute joints. The complete structural model involved 5,656 states.

The aerodynamic modeling combines thin airfoil theory with a three dimensional dynamic inflow model. The inflow velocities at each span-wise location were computed using the finite state induced flow model developed by Peters *et al.* [18, 19]. The airfoil has a constant slope of the lift curve $a_0 = 5.73$, and drag coefficient $c_d = 0.018$; the moment coefficients about the quarter-chord are zero. The number of inflow harmonics was selected as $m = 10$, corresponding to 66 aerodynamic inflow states. Airloads were computed at 81 equally spaced stations along the quarter-chord line of each blade.

The goal of this study is to trim the rotor, *i.e.* to find the collective blade angle for which the rotor thrust achieves a target value of $L_t = 17,944$ lbs. The trimming process is seen as a two step operation. At first, a plant model is identified, which accurately captures the input-output behavior of the system: the system input is the collective angle, whereas the system output is the rotor thrust. The proposed robust system identification algorithm is used for this purpose. Next, once a linearized model about a possibly time dependent equilibrium configuration of the nonlinear rotor system is constructed, a linear quadratic Gaussian controller was implemented to trim the rotor.

System identification was performed as follows: at first, a dynamic simulation was run for a total period of 3.488 sec using a constant time step $\Delta t = 1.8167$ msec. The collective blade angle, θ, and rotor lift L, were selected as control input and output, respectively. The initial value of collective angle was set as $\theta_0 = 0.1$ rad and the corresponding mean value of the lift was found to be $L_m = 8,960.20$ lbs. Next, the collective angle was perturbed for a period of 0.5 sec as $\Delta\theta = \pi/20\ (1 - \cos(4\pi(t - 1.0)))$ for $t \in [1.0,\ 1.5]$ sec and $\Delta\theta = 0$ for $t > 1.5$ sec; this perturbation is shown on the top portion of fig. 4. The response of the system to an impulse input was determined by computing the

difference between the perturbed lift and its reference counterpart. The system identification algorithm was applied to the response of the system over the time window $t \in [1.0,\ 3.44]$ sec to construct a 12^{th} order forward innovation model. The outputs of the full and identified models were evaluated and are shown in fig. 4; a good correlation between the two models is observed.

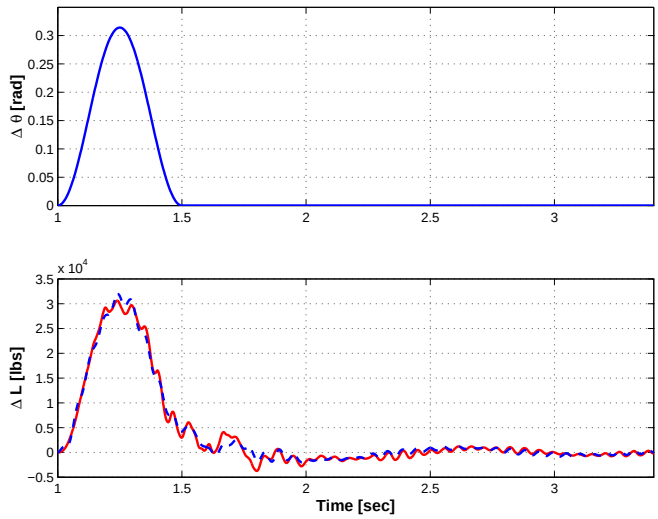

Figure 4: Top figure: time history of the control input. Bottom figure: system output computed using the full model (solid line) and the identified 12^{th} order plant model (dashed line).

Once a reduced order plant model was identified, a linear quadratic Gaussian controller was used to trim the rotor to its target thrust of $L_t = 17,944$ lbs. Figure 5 shows the time history of the control input and output; the controller becomes active 1 sec into the simulation. The proposed approach to trimming quickly identified the control settings, although a low frequency oscillation remains in the output signal. This is probably due to the fact that the identification was performed over too short a window, which did not allow proper identification of the slowest modes of the system.

5 Conclusions

Comprehensive approaches for stability analysis and system identification of flexible multibody systems have been investigated. A new system identification algorithm was implemented as an extension of stability analysis methodologies. The approach only requires input and output data from the system, and hence, it is well suited for solving multibody, multi-physics problem.

The proposed system identification algorithm uniquely combines the methods of minimum realization and subspace identification. For minimum realization, the computation of Markov parameters remains complex and determines the

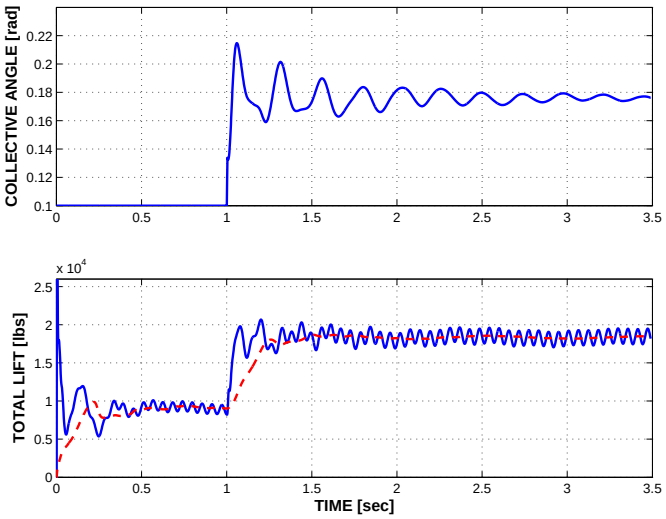

Figure 5: Top figure: time history of the control input computed by the controller. Bottom figure: total instantaneous thrust of the rotor (solid line), and moving average (dashed line).

accuracy of the system realization. The proposed approach bypasses the computation of Markov parameters because the free impulse response of the system can be directly computed in the present computational environment. Minimum realization concepts were applied to identify the stability and output matrices. On the other hand, subspace identification algorithms construct a state space plant model of linear system by using computational expensive oblique matrix projection operations. The proposed algorithm avoids this burden by computing the Kalman filter gain matrix and model dependency on external inputs in a small sized subspace. The robustness of this algorithm was improved by the application of the singular value decomposition and least squares regression techniques.

The proposed approach allows the identification of both deterministic and stochastic-deterministic models. Numerical results were presented that demonstrate the robustness and accuracy of the proposed approach.

References

[1] C.H. Kim and J.S. Arora. Nonlinear dynamic system identification for automotive crash using optimization: A review. *Structural and Multidisciplinary Optimization*, 25(1):2–18, 2003.

[2] M. Viberg. Subspace-based methods for the identification of linear time-invariant systems. *Automatica*, 31(12):1835–1851, 1995.

[3] E.R. Kalman. Mathematical description of linear dynamical systems. *SIAM Journal on Control*, 1(2):152–192, 1963.

[4] B. Ho and R. Kalman. Efficient construction of linear state variable models from input/output functions. *Regelungstechnik*, 14:545–548, 1966.

[5] B.C. Moore. Principal component analysis in linear systems: Controllability, observability, and model reduction. *IEEE Transaction on Automatic Control*, AC-26(1):17–32, 1981.

[6] J.N. Juang and R.S. Pappa. An eigensystem realization algorithm for modal parameter identification and model reduction. *Journal of Guidance, Control, and Dynamics*, 8(5):620–627, 1985.

[7] P. Overschee and B. De Moor. *Subspace Identification for Linear Systems: Theory-Implementation-Applications*. Springer, New York, New York, 1996.

[8] B. Peeters and G. De Roeck. Stochastic system identification for operational modal analysis: A review. *ASME Journal of Dynamic Systems, Measurement, and Control*, 123:659–667, 2001.

[9] S. Lall, J.E. Marsden, and S. Glavaški. A subspace approach to balanced truncation for model reduction of nonlinear control systems. *International Journal of Robust and Nonlinear Control*, 12(5):519–535, 2002.

[10] O.A. Bauchau and J.L. Wang. Stability analysis of complex multibody systems. *Journal of Computational and Nonlinear Dynamics*, 1(1):71–80, January 2006.

[11] O.A. Bauchau and J.L. Wang. Efficient and robust approaches to the stability analysis of large multibody systems. *ASME Journal of Computational and Nonlinear Dynamics*, 2007. To appear.

[12] G.H. Golub and C.F. Van Loan. *Matrix Computations*. The Johns Hopkins University Press, Baltimore, second edition, 1989.

[13] J.N. Juang. *Applied System Identification*. Prentice-Hall, Inc., Englewood Cliffs, New Jersey, 1994.

[14] W.F. Arnold and A.J. Laub. Generalized eigenproblem algorithms and software for algebraic Riccati equations. *Proceedings of the IEEE*, 72(12):1746–1754, 1984.

[15] J.W. Brewer. Kronecker products and matrix calculus in system theory. *IEEE Transaction on Circuits and Systems*, 25(9):772–781, 1978.

[16] O.A. Bauchau, C.L. Bottasso, and Y.G. Nikishkov. Modeling rotorcraft dynamics with finite element multibody procedures. *Mathematical and Computer Modeling*, 33(10-11):1113–1137, 2001.

[17] W.G. Bousman and T. Maier. An investigation of helicopter rotor blade flap vibratory loads. In *American Helicopter Society 48th Annual Forum Proceedings*, pages 977–999, Washington, D.C., June 3-5 1992.

[18] D.A. Peters, S. Karunamoorthy, and W.M. Cao. Finite state induced flow models. Part I: Two-dimensional thin airfoil. *Journal of Aircraft*, 32(2):313–322, 1995.

[19] D.A. Peters and C.J. He. Finite state induced flow models. Part II: Three-dimensional rotor disk. *Journal of Aircraft*, 32(2):323–333, 1995.